Androgens inhibit the osteogenic response to mechanical loading in adult male mice

Mieke Sinnesael[1], Michaël R. Laurent[2,3], Ferran Jardi[1], Vanessa Dubois[2], Ludo Deboel[1], Peter Delisser[4], Geert J. Behets[5], Patrick C. D'Haese[5], Geert Carmeliet[1], Frank Claessens[2], and Dirk Vanderschueren[1]

[1] Clinical and Experimental Endocrinology, Department of Clinical and Experimental Medicine, KU Leuven, Leuven, Belgium; [2] Molecular Endocrinology Laboratory, Department of Cellular and Molecular Medicine, KU Leuven, Leuven, Belgium; [3] Gerontology and Geriatrics, Department of Clinical and Experimental Medicine, KU Leuven, Leuven, Belgium; [4] School of Veterinary Science, University of Bristol, Bristol, United Kingdom; [5] Laboratory of Pathophysiology, University of Antwerp, Antwerp, Belgium

Key terms: Androgens, sclerostin, bone, osteocyte, loading

Androgens are well known to enhance exercise-induced muscle hypertrophy, however whether androgens also influence bone's adapative response to mechanical loading remains unclear. We studied the adaptive osteogenic response to unilateral *in vivo* mechanical loading of tibia in adult male mice in both a long and a short term experimental set-up. Mice were divided in 4 groups: sham-operated, orchidectomized (ORX), testosterone (ORX+T) or non-aromatizable dihydrotestosterone (ORX+DHT) replacement. Significant interactions between androgen status and osteogenic response to mechanical loading were observed. Cortical thickness increased by T (0.14 *vs.* 0.11 mm sham, $p<0.05$) and DHT (0.17 *vs.* 0.11 mm sham, $p<0.05$). However, T partially (+36%) and DHT completely (+10%) failed to exhibit the loading-related increase observed in sham (+107%) and ORX (+131%, all $p<0.05$) mice. ORX decreased periosteal bone formation (PsBFR), which was restored to sham levels by T and DHT. However, both androgens completely suppressed the loading-related increase in PsBFR. Short term loading decreased the number of sclerostin positive osteocytes in sham, whereas in control fibulas, ORX decreased and T increased the number of sclerostin positive osteocytes. Loading no longer downregulated sclerostin in ORX or T groups.

In conclusion, both T and DHT suppress the osteogenic response to mechanical loading.

Osteoporosis in men is less frequent than in postmenopausal women, yet still represents an undertreated condition with a considerable burden for patients and society (1). Others and we recently showed that antiresorptive therapy prevents fractures in osteoporotic men, apparently with similar efficacy as seen in women (2). However, a considerable proportion of subjects treated with powerful antiresorptives will continue to fall and fracture. Thus, there remains an unmet need for musculoskeletal anabolic therapies in both genders but potentially more so in elderly osteoporotic men, in whom decreased bone formation, sarcopenia and frailty appear to play a greater role than in postmenopausal osteoporosis (3). Androgens and selective androgen receptor modulators are potential treatments for frail elderly men at risk for fractures (4). Frailty in older men is associated not only with sarcopenia but also lower testosterone (T) levels (5). Moreover, late-onset male hypogonadism is associated with decreased bone density, impaired bone architecture and increased fracture risk (6–9). The diagnosis and management of late-onset male hypogonadism remains controversial (10) yet prescription rates of T in this indication are rising (11), despite concerns about cardiovascular side effects of T replacement in frail older men (12). The effects of T on the male skeleton, either directly via the androgen receptor (AR) or indirectly as the substrate for aromati-

ISSN Print 0013-7227 ISSN Online 1945-7170
Printed in U.S.A.

Received August 11, 2014. Accepted February 2, 2015.

Abbreviations:

zation into estrogens acting via estrogen receptor alpha (ERα), continues to be debated (13). Substudies from the trial by Finkelstein et al (14) as well as the NIH-sponsored Testosterone Bone Trial (15) will hopefully shed light on this issue in the near future. Given the well-known anabolic actions of T on muscle however (14, 16) and its importance for male skeletal conservation (13), androgens could in principle be of great interest to simultaneously ameliorate both skeletal and extra skeletal determinants of fracture like muscle mass, falls and frailty (17).

Bone adapts its microarchitecture not only to endocrine stimuli but also to mechanical loading (18). According to Frost's mechanostat theory, mechanical stress that results in strain above habitual levels will result in adaptations in bone structure to reduce local strains by changing bone remodeling, resulting in greater bone formation than resorption (19). The osteoanabolic effects of physical exercise are evident in elite athletes eg, in the dominant arm of tennis players (20). Several studies have suggested that changes in the endocrine environment such as during puberty, aging or after menopause may affect the osteogenic response of bone (21, 22). In humans however, it is difficult to study the effects of sex steroids on bone's adaptive loading response to exercise independent of muscle-bone interactions. Mouse models with direct in vivo skeletal loading allow mechanistic elucidation of these effects, independent of muscle. A landmark study from the group of Lanyon showed that mechanoresponsiveness was diminished in female ERα knock-out (ERαKO) mice (23). Recent studies showed that this effect occurs in a ligand-independent manner involving activation function 1 (AF-1) in the N-terminal domain of ERα (24). Conflicting results showing enhanced or unaltered osteogenic responses were however obtained in male ERαKO mice (25, 26). We previously showed that male AR knock-out (ARKO) mice, which display a low periosteal bone formation (27), unexpectedly showed a greater response to in vivo mechanical ulna loading (25). However, this study had some limitations including the absence of the androgen receptor (AR) and low levels of T (which is also the substrate for aromatization) from early life on in ARKO mice (ie, developmental disturbances), the inability to judge whether absence of ligands contributes to this effect, or the response of trabecular bone in the ulna vs. tibia loading model. The in vivo interactions of androgens and mechanical loading with pathways that respectively control bone formation (such as Wnt signaling) or bone resorption (such as RANKL/OPG) also remain unclear. Thus, the aim of this study was to examine the interaction of androgen status with the osteogenic response to mechanical loading in a preclinical model of adult male mice with acquired sex steroid deficiency and T or nonaromatizable dihydrotestosterone (DHT) replacement. Moreover, effects following long- as well as –short term loading were assessed.

Materials and Methods

Animals

Male C57BL/6 mice were purchased from Charles River Laboratories and group-housed in conventional conditions: 12-hour light/dark cycle, standard diet (1% calcium, 0.76% phosphate), water ad libitum in standard cages. The Ethical Committee of the KU Leuven approved all procedures (P143/2011).

Experimental design

At 16 weeks of age, animals were either sham-orchidectomized (sham), orchidectomized (ORX), orchidectomized with T replacement silastic (ORX+T) or orchidectomized with DHT replacement (ORX+DHT). DHT (Fluka Chemika, Buchs, Switzerland) and T (Serva, Heidelberg, Germany) were administered using subcutaneous silastic implants (Silclear Tubing, Degania Silicone, Jordan Valley, Israel) in the cervical region as described in previous studies (27–29). T or DHT were administered immediately after ORX. The daily dose of T administered by 1 cm silastic is 23 μg while the 1.5 cm DHT silastic has a release of 45 μg/d. Sham-treatment animals received empty implants. Efficacy of ORX and hormone replacement was verified by measurement of seminal vesicle wet weight immediately after euthanasia. Androgen dosage was slightly supraphysiological, as indicated by the higher seminal vesicle weight in ORX+T and ORX+DHT groups compared to sham surgery group (Table 1). Loading of the right tibia started either 1 or 10 days after surgery to study the long term effects of external mechanical stress (Figure 1 upper part and Supplemental Figure 1) (30). In another experiment, the right tibia was subjected to loading only once in order to assess the short term response (Figure 1 lower part). The left tibia served as internal control. Calcein (16 mg/kg, Sigma Chemical Co., St. Louis, MO, USA) was injected intraperitoneally 5 and 1 day before euthanasia.

In vivo tibia mechanical loading

Mice were anesthetized with isoflurane during which time the flexed knee and ankle joints were positioned in concave cups; the upper cup, into which the knee was positioned, was attached to the actuator arm of a servo-hydraulic loading machine (ElectroForce 3100 Test Instrument, Bose Corp.) and the lower cup to a dynamic load cell. The right tibia was held in place by a low level of continuous static preload, onto which higher levels of intermittent "dynamic" load were superimposed. In the current study, 16.5N dynamic load and 2.0N static preload were applied in a series of 40 trapezoidal-shaped pulses (0.025 seconds loading, 0.050 seconds hold at 16.5N, and 0.025 seconds unloading) with a 10-second rest interval between each pulse. Left tibias served as internal controls (31). Three different experimental designs were used. In a first experiment, 16-week-old mice were ORX and immediately given androgen replacement (T or DHT) or vehicle. After 10 days recovery, loading was given three times a week on alternate days for two weeks (Figure 1 upper part) (30). On day 22 and 25 mice were injected with calcein to assess

Table 1. Effects of androgens on general parameters and on control, non-loaded limbs at the end of the long term experiment (19 wk of age)

	SHAM	ORX	ORX+T	ORX+DHT
BW (g)	29 ± 1	29 ± 1	31 ± 2	30 ± 1
SV (mg)	347 ± 24	53 ± 7 [b]	387 ± 20	373 ± 24
SV/ BW (mg/ 100g)	1184 ± 80	185 ± 20 [b]	1264 ± 91	1252 ± 87
Tibia Length (mm)	18.3 ± 0.1	18.2 ± 0.1	18.3 ± 0.1	18.2 ± 0.1
Ct.Ar (mm^2)	0.99 ± 0.04	0.91 ± 0.02	0.99 ± 0.04	0.92 ± 0.03
Ct.Th (mm)	0.11 ± 0.01	0.09 ± 0.001	0.14 ± 0.01 [a,b]	0.17 ± 0.003 [a,b]
Ps.BFR/ B.Pm. ($\mu m^2/\mu m$/DAY)	0.67 ± 0.11 [a]	0.07 ± 0.01	0.42 ± 0.04 [a,b]	0.61 ± 0.15
Ec.BFR/ B.Pm. ($\mu m^2/\mu m$/DAY)	0.40 ± 0.12	0.31 ± 0.14	0.15 ± 0.04	0.52 ± 0.06 [a,c]
BV/TV (%)	7.4 ± 0.4 [a]	2.3 ± 0.4	13.5 ± 1.1 [a,b]	10.8 ± 0.4 [a,b,c]
Tb.Th (mm)	0.049 ± 0.003	0.047 ± 0.002	0.044 ± 0.002	0.035 ± 0.001[a,b,c]
Tb.N (mm^{-1})	2.06 ± 0.41 [a]	0.47 ± 0.08	3.06 ± 0.24 [a,b]	3.05 ± 0.09 [a,b]
Tb.Sp (mm)	0.26 ± 0.03 [a]	0.55 ± 0.07	0.20 ± 0.01 [a]	0.21 ± 0.002 [a]
Tb.BFR ($\mu m^2/\mu m$/DAY)	0.68 ± 0.05 [a]	1.12 ± 0.15	0.24 ± 0.07 [a,b]	/

1

[1]Body weight (BW), seminal vesicle weight (SV) and SV/BW were measured at sacrifice after 2 weeks of loading, as described in material and methods. Tibia length, cortical area (Ct.Ar), cortical thickness (Ct.Th), periosteal bone formation rate per bone perimeter (Ps.BFR/B.Pm.), endocortical bone formation rate per bone perimeter (Ec.BFR/B.Pm.), BV/TV, trabecular thickness (Tb.Th), trabecular number (Tb.N), trabecular separation (Tb.Sp) and trabecular bone formation (Tb.BFR) were measured in the left tibia (control). Values are expressed as means ± SD, n = 7–11 mice/group. [a]$P < 0.05$ *vs.* ORX, [b]$P < 0.05$ *vs.* SHAM, [c]$P < 0.05$ *vs.* ORX+T.

bone formation. After 24 hours, mice were euthanized and left and right tibias were used for μCT and bone formation assessment, hereby investigating the long term effects of loading. In a second experimental set-up the short term effects of loading were determined (Figure 1 lower part). 19-week-old mice were divided again in 4 groups although now the right tibia was loaded only once 1 day after surgery (using the same loading parameters as the long term set-up). The left tibia served as internal control. 24 hours later mice were euthanized and left and right tibias were used for *Rankl*/*Opg* mRNA expression. Sclerostin immunohistochemistry was performed in both left and right fibulas and terminal serum was used for sclerostin detection. In the third experiment, 16-week-old mice were subjected to mechanical loading starting on the day following surgery (Supplemental Figure 1). Right tibias were loaded for 2 weeks on alternate days (using the same loading parameters as the long term set-up) whereas left tibias served as internal controls. At day 16, mice were euthanized and left and right tibias were used for μCT.

Strain gauges attached to the medial proximal tibial shaft, 35%-40% of the length of the bone measured from the proximal end in similar 17-week-old male C57BL/6 mice showed that a peak load of 16.5 N engendered approximately 2250 microstrain in that region and was not significantly different between the 4 groups.

High-resolution microcomputed tomography (μCT) analysis

The tibiae from both hind limbs were collected after euthanasia, stored in 70% ethanol, and scanned by μCT (SkyScan 1172; Bruker, SkyScan, Kontich, Belgium) with a resolution of 5 μm. Images of the bones were reconstructed using NRecon software. Analyses were undertaken for trabecular (secondary spongiosa, 0.25–0.75 mm distal to the growth plate) and cortical bone (0.5-mm-long section at 37% of the bone's length from its proximal end). At these trabecular and cortical sites, the loading regimen used in the present study has previously shown to increase bone volume (32). The parameters evaluated in the trabecular region included bone volume/tissue volume (BV/TV, %), trabecular thickness (Tb.Th, mm), trabecular number (Tb.N, mm^{-1}) and trabecular separation (Tb.Sp, mm). In the cortical region cortical area (Ct.Ar, mm^2), cortical thickness (Ct.Th,

mm), periosteal perimeter (PsPm, mm), endocortical perimeter (EcPm, mm), medular area (Me.Ar, mm^2), crossectional area (Csa, mm^2), mean polar moment of inertia (MPMI, mm^4) and porosity (Poro, %) were determined as previously reported (33–35).

Long term dynamic and static bone histomorphometry

Bone formation rate (BFR) at the periosteal and endosteal surfaces of the cortical bone in the mid-diaphyseal region of the tibia were evaluated by dynamic histomorphometric analyses after the long term loading effect protocol. Tibiae were fixed in Burckhardt's fixative (24 hours, 4°C), kept in ethanol, and embedded in methyl methacrylate. Cross sections of the undecalcified tibiae perpendicularly to the long axis were prepared at 200 μm thickness in the middiaphyseal region using the contact-point precision band saw (Exakt, Norderstedt, Germany). Sections were ground to a final thickness of 25 μm using a grinding system (Exakt), left unstained, and subjected to dynamic histomorphometry. Three sections in the middiaphyseal region were measured by fluorescence microscopy, and the bone formation rate (BFR, $\mu m^2/\mu m$/ day) was assessed at both the endocortical and periosteal bone surfaces. The BFR was obtained by the product of mineral apposition rate (MAR, μm/d) and mineralizing perimeter per bone perimeter (Min.Pm./B.Pm., %). The mineralizing perimeter was calculated as follows: Min.Pm.=[dL + (sL/2)]/B.Pm., where dL represents the length of the double labels, and sL is the length of single labels along the entire endocortical or periosteal bone surfaces. The MAR (μm/d) was calculated as the mean width of double labels divided by interlabel time. For assessment of trabecular bone formation left and right tibiae were fixed in Burkhardt's solution, embedded undecalcified in methyl methacrylate, and sectioned at 4 μm. Unstained sections were used to analyze calcein labeling. Histomorphometric analysis was done as described previously (36). All measurements were performed with a Kontron Image Analyzing Software (KS400 3.00; Kontron Bildanalyze, Munich, Germany) and a Zeiss microscope with a drawing attachment. Specific software was developed in collaboration with the manufacturer. Histomorphometric parameters are reported according to the recommended American Society for Bone and Mineral Research nomenclature (37).

Osteoclast parameters were determined in 4 μm-thick Goldner-stained longitudinal sections of the tibia. The slides were viewed under a Leica DMRB microscope (Leica Microsystems, Wetzlar, Germany) equipped with a digital camera (Axiocam HRc, Carl Zeiss Microscopy, Jena, Germany) and analyzed using image analysis software (Axiovision Version 4.5, Carl Zeiss Microscopy, Jena, Germany) running in-house developed software. Digital images of adjacent fields (original magnification 200x) were taken until the whole section was analyzed. The trabecular bone, eroded and osteoclast perimeters were marked by the operator and afterwards the system calculated the relative percentages.

Short term sclerostin immunohistochemistry

Mice of 19 weeks of age were subjected to a single loading the day after surgery, to study the short term effects. The fibulae of both hind limbs were collected 24 hours after one loading and used for cortical osteocytic immunohistochemistry (38). The same loading parameters were used as in the long term loading protocol. Bones were dissected of soft tissue and fixed in 10% formalin. Sclerostin was immunolocalized at the proximal sites in decalcified, wax-embedded 8-μm transverse sections using an indirect immunoperoxidase method (39). Goat polyclonal antimouse sclerostin (0.2 mg/ml; R&D Systems, Abingdon, UK) and biotinylated rabbit anti-goat (0.013 mg/ml; Dako, Ely, UK) were used as the primary and secondary antibodies, respectively. All antibodies were diluted in 10% rabbit serum (Sigma Chemical Co.) in calcium and magnesium-free phosphate buffered saline (Gibco, Paisley, UK). The same concentration of goat IgG was substituted for the primary antibody as a negative control. Detection of sclerostin was carried out using vector ABC kit (Vector Laboratories, Burlingame, USA) with diaminobenzidine as a substrate. 1% light green solution was used as background staining. The immunolabeled sections were photographed with a Kontron Im-

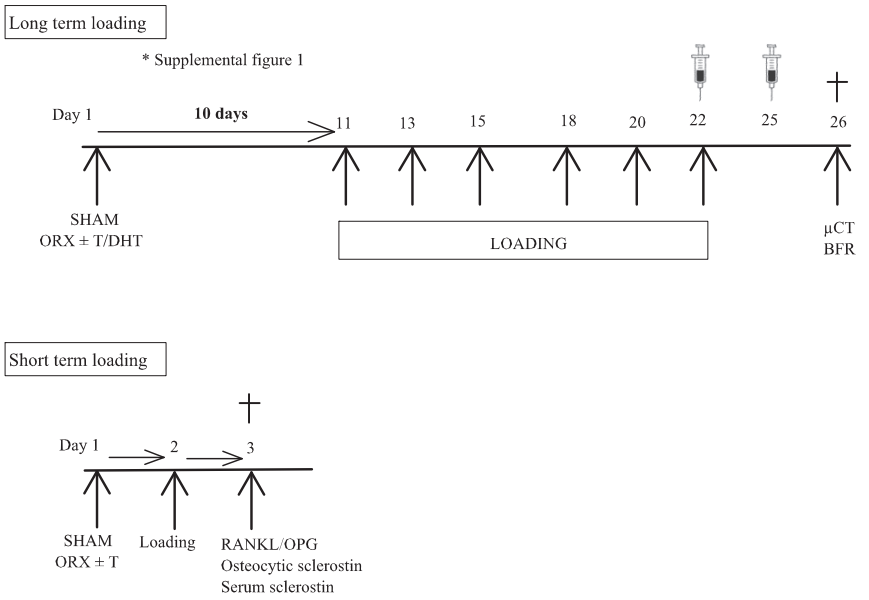

Figure 1. Overview of experimental designs. 16-week-old mice were sham, ORX, ORX+T or ORX+DHT on day 1. External mechanical loading of the right tibia was initiated 10 days after surgery to study the long term effects of mechanical loading (upper part). The left tibia was used as internal control. Mice were injected with calcein on day 22 and day 25 (as shown by syringe). At day 26 mice were euthanized and left and right tibia were analyzed with μCT and cortical as well as trabecular bone formation was assessed. External mechanical loading of the right tibia was initiated 1 day after surgery in order to study the short term effects of loading (lower part). 19-week-old mice were again divided in the four groups (sham, ORX, ORX+T and ORX+DHT). The left tibia was used as internal control. At day 3 (24 hours after one single loading) mice were euthanized and left and right tibias were used to assess *Rankl*/*Opg* mRNA expression. Left and right fibula were used for sclerostin immunohistochemistry and terminal serum for sclerostin detection. n = 7–11 per group for both loading set-ups.

age Analyzing Software (KS400 3.00; Kontron Bildanalyze, Munich, Germany) and a Zeiss microscope with a drawing attachment. The number of sclerostin-positive osteocytes (brown staining) and sclerostin-negative osteocytes (green staining) were counted in a standardized area on each section (8 to 10 sections per mouse) using ImageJ software. The percentage sclerostin-positive cells was calculated as the number of sclerostin-positive osteocytes divided by the total number of osteocytes (positive+negative). Calculations were performed on the lateral axis, where the strain is the highest in the fibula (38, 40, 41), as well as in the total fibula. Since the results did not differ according to the region of measurement results were expressed for the total fibula.

Short term Rankl/Opg expression

To study the rapid changes due to mechanical loading, mice at 19 weeks of age were subjected to a single loading the day immediately after surgery. The tibiae of both hind limbs were carefully dissected 24 hours after one single loading and all their surrounding musculature removed. The cartilaginous ends of the bones were removed and tibial shafts were then snap-frozen in liquid nitrogen, pulverized under liquid nitrogen using a mortar and pestle and lysed in Qiazol lysis reagent (Qiagen Ltd., Crawley, UK). cDNA was synthesized from DNaseI-treated total RNA (RNeasy Kit, Qiagen, Hamburg, Germany) by using superscript II RNaseH$^-$ reverse transcriptase and random hexamer primers (Invitrogen, Ghent, Belgium). Primers and probe used for *Rankl*: forward primer: 5′ -CATTTGCACACCTCACCATCA-3′; reverse primer: 5′-TTGCTTAACGTCATGTTAGAGATCTTG-3′; probe: 5′ -TCGGGTTCCCATAAAGTCACTCTG TC-CTCTT-3′ (amplicon = 118 bp); *Opg*: forward primer: 5′ -GAAGGGCGTTACCTGGAGATC-3′; reverse primer: 5′ -CT-GAATTAGCAGGAGGCCAAAT-3′; probe: 5′ -TCACCT-GAGAAGAACCCATCTGGACATTTT-3′ (amplicon = 201 bp). For quantification of gene expression, the ABI Prism 7500 sequence detector PCR detection system (Applied Biosystems, Ghent, Belgium) was used with a two-step RT-quantitative PCR protocol. The relative expression levels of the target genes were calculated as a ratio to the HPRT gene with the following primers and probe: forward primer: 5′ -TTATCAGACTGAAGAGC-TACTGTAATGATC-3′; reverse primer: 5′ -TTACCAGTGT-CAATTATATCTTCAACAATC-3′; probe: 5′ -TGAGAGAT-CATCTCCACCAATAACTTTTAT GTCCC-3′ (amplicon = 127 bp).

Short term serum sclerostin

Serum sclerostin of 19 week-old mice that were loaded once was measured after 24 hours by a mouse/rat sclerostin quantikine ELISA kit according to the manufacturer's instructions (R&D systems Europe, Oxon, UK)

Statistical analysis

Statistical analysis was performed using NCSS software (NCSS, Kaysville, UT, USA). Repeated measures two-way analysis of variance (ANOVA) was performed to assess the effect of androgens, loading and interaction between both interventions, followed by Fisher's least significant differences multiple comparison test. Interaction was defined as $p \leq 0.15$ (42). Student's *t* test or one-way ANOVA followed by Fisher's least significant difference multiple comparison test were performed to assess difference between two or more groups, respectively. Data are represented as means ± standard deviation, and a two tailed p value < 0.05 was accepted as significant.

Results

Effects of androgens

The seminal vesicle weight, body weight, tibia length, μCT and dynamic bone formation parameters of the control tibia were measured after a 10-day interval followed by two weeks of loading. Body weight (43), tibia length and cortical area were not different between groups (Table 1). Seminal vesicle weight/body weight in ORX was significantly reduced compared to sham. In internal control, cortical thickness was significantly increased with T and DHT replacement when compared to sham or ORX. As expected, trabecular bone volume decreased following ORX, vs sham (2.3 vs. 7.4%, $P < .05$), *as a result of reduced trabecular number (0.47 vs.* 2.06 mm^{-1}, $P < .05$) *but not thickness (0.047 vs.* 0.049 mm). DHT and even more efficiently T replacement increased trabecular bone volume (ORX+DHT 10.8; ORX+T 13.5%, $P < .05$) above sham (7.4%) levels in respectively ORX+DHT and ORX+T mice. This effect was also secondary to an increase of trabecular number (ORX+DHT 3.05; ORX+T 3.06 mm^{-1}, $P < .05$). *Trabecular separation was increased by ORX compared to sham (0.55 vs.* 0.26 mm, $P < .05$) *and reduced again by DHT as well as T vs ORX (DHT 0.21, T 0.20 vs.* 0.55, $P < .05$) (Table 1).

Long term loading induced μCT changes

Loading increased cortical thickness in sham (+107%), ORX (+131%) and ORX+T (+36%) mice (Figure 2A and B). This loading induced increase was greater in ORX animals and inhibited by T and even more by DHT. Loading increased trabecular volume and reduced separation in sham because of both higher number and thickness of trabeculae (Supplemental Figure 2). This loading-induced increase was significantly higher in ORX animals. T and DHT replacement attenuated this response to loading-induced gain of trabecular bone volume. Neither of the treatments nor their interaction produced changes in the cortical or trabecular volumetric bone mineral density (BMD) (Supplemental Table 1 and Supplemental Figure 2).

Long term effect on bone formation and osteoclast parameters

Periosteal bone formation rate was lower in control ORX (0.07 $\mu m^2/\mu m$/DAY) than sham (0.67 $\mu m^2/\mu m$/DAY) and ORX+T (0.42 $\mu m^2/\mu m$/DAY) and

ORX+DHT (0.61 $\mu m^2/\mu m$/DAY) (Table 1 and Figure 3) due to both lower periosteal mineralizing perimeter and periosteal mineralizing apposition rate. Periosteal bone formation rate increased by loading in sham (+170%, $P <$ .05), even further in ORX (+732%, $P < .05$) but not in ORX +T (+8%, not significant) or in ORX+DHT (-85%, $P < .05$). Trabecular bone formation rate was higher in control ORX (1.12 $\mu m^2/\mu m$/DAY) but lower following T (0.24 $\mu m^2/\mu m$/DAY) vs sham (0.68 $\mu m^2/\mu m$/DAY) (Supplemental Table 2). Trabecular bone formation rate increased substantially by loading in sham (+44%, $P < .05$) and in ORX (+42%, $P < .05$) but far less in ORX+T (+6%, n.s.). Endocortical bone formation rates tended to be lower in control ORX (0.31 $\mu m^2/\mu m$/DAY) and in ORX+T (0.15 $\mu m^2/\mu m$/DAY) compared to sham (0.40 $\mu m^2/\mu m$/DAY) (Table 1). Endocortical bone formation increased after loading in sham (+90%, $P <$ .05), ORX (+108%, $P < .05$), ORX+T (+60%, n.s.) and decreased in ORX+DHT (-48%, $P < .05$) (Supplemental Table 2).

We observed an increase in osteoclast parameters (eroded perimeter and osteoclast perimeter per bone or eroded perimeter) after ORX, which was totally prevented by T replacement (Figure 4). Loading also tended to increase erosion values but only within ORX group, reaching statistical significance for osteoclast perimeter per bone perimeter (+87%, $P < .05$).

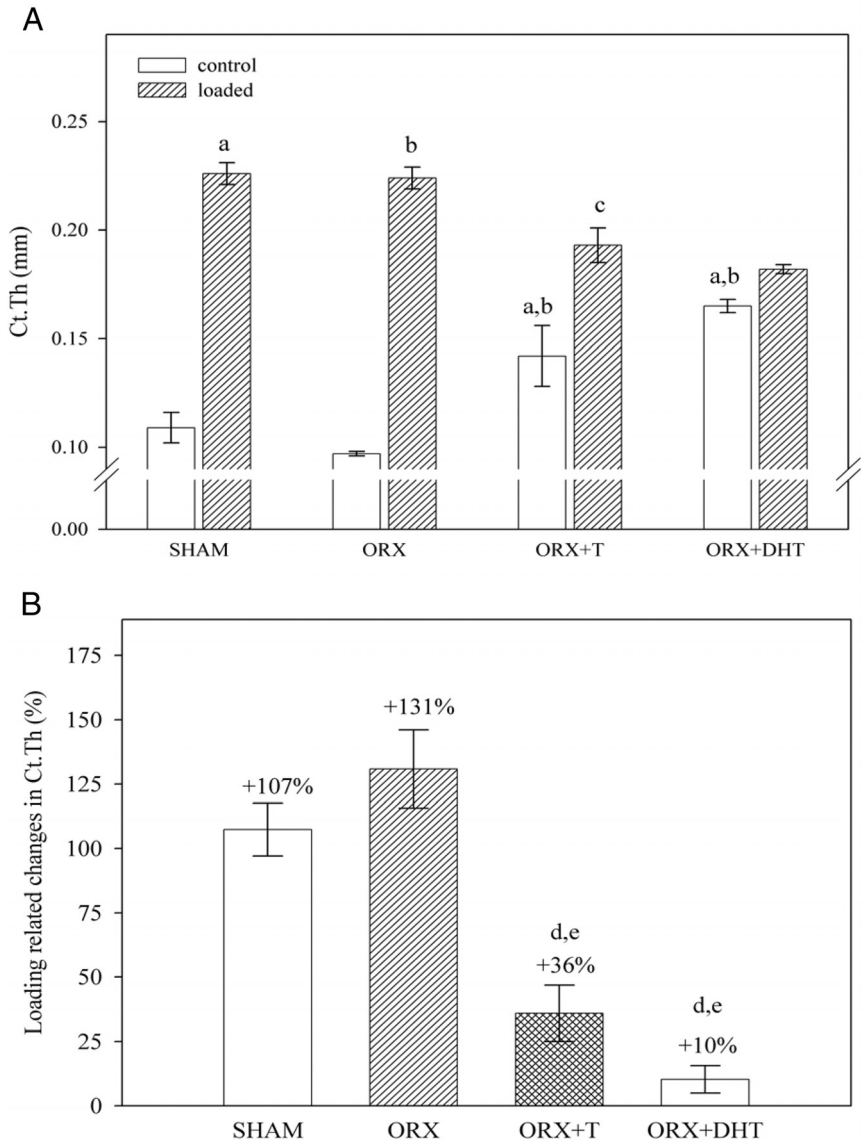

Figure 2. Long term loading-induced changes measured by ex vivo μCT. Cortical thickness (Ct.Th) in sham, ORX, ORX+T and ORX+DHT mice. A, Absolute values and (B) relative loading-related changes ((right loaded-left control)/left control)*100 of Ct.Th. Values are expressed as means ± SEM, n= 7–11 mice/group. $^aP < .05$ vs sham control, $^bP < .05$ vs ORX control, $^cP <$ .05 vs ORX+T control by Repeated measures ANOVA to assess interaction between treatment and loading followed by Fisher's least significant differences multiple comparison test.

Short term effect on *Rankl/Opg*

The right tibia was loaded once in order to study short term changes caused by mechanical loading. RNA was isolated 24 hours later. *Rankl/Opg* ratio increased in control ORX (+118%, $P < .05$) as well as in ORX+T (+45%, $P < .05$) vs sham. Loading significantly reduced *Rankl/Opg* ratio in ORX (-52%, $P <$ .05) (Figure 5) secondary to an increase in *Opg* and no change in *Rankl*. *Opg* did not increase in ORX+T due to loading although *Rankl* decreased significantly in this group.

Short term effect on osteocytic sclerostin expression and circulating sclerostin

Loading resulted in a significant reduction in the number of sclerostin positive osteocytes in sham (-65%, $P < .05$) (Figure 6A) 24 hours after one single loading. However, in control fibulas, sclerostin positive osteocytes were significantly reduced in ORX (-40%, $P < .05$) and increased in ORX+T (+27%, $P < .05$) vs sham and showed no response to loading. Serum sclerostin was significantly decreased in loaded sham (-33%, $P < .05$) and in ORX (- 22%, $P < .05$) (Figure 6C). However there was no correlation between osteocytic sclerostin and serum sclerostin.

Discussion

The main finding of this study is that acquired androgen deficiency elicits cortical and trabecular bone loss but enhances the osteogenic response to loading, whereas exogenous replacement decreased the mechanoresponsiveness in this hypogonadal male mouse model. Our findings may seem counterintuitive yet confirm and extend earlier observations of increased osteogenic response to loading in male mice with either sex steroid deficiency and/or sex steroid receptor disruption. In a previous study, loading of ORX mice led to a higher increase of cancellous bone volume, trabecular thickness and mineral apposition rate compared to sham mice, but whether this was due to loss of androgens, estrogens or both was not confirmed with replacement conditions (44). T has a well-established dual mode of action through both AR and ERα in male mice (45). In the present study, DHT produced equal or even stronger (Figure 2 and Figure 3) inhibition of bone formation compared to T during loading, indicating a direct role for AR activation. We previously showed that loading induced greater periosteal bone formation in ARKO mice as well as male mice with combined AR and ERα disruption (AR-ERα KO) compared to WT mice (25). Net-osteogenic response to loading has been shown to be greater in male ERαKO mice in one study (26), whereas no effect of ERα disruption was observed in another study (25). This could be explained by disturbed hypothalamic feedback in both studies and residual ligand responsiveness via ERα AF-2 in the Korach's ERαKO model. In earlier mice studies, the response to mechanical stimulation in female mice was shown to be mediated independent of estrogens, via the N-terminal AF-1 domain of ERα (24). In the present study, the absence of loading response in both the cortical and cancellous compartments was mediated by circulating androgens. In addition, the observed changes in mechanoresponsiveness following androgen deficiency are the same as observed in ARKO mice (25), therefore AR-mediated effect seems to be a ligand-dependent effect.

The observed interaction between androgens and mechanical loading is likely not explained via divergent effects on the RANKL/OPG system, since we only observed a significant decrease in *Rankl/Opg* ratio after castration. The Wnt/β-catenin pathway on the other hand is crucial for the osteogenic pathway as seen in response to loading. Sclerostin is a Wnt inhibitor produced by osteocytes and a powerful inhibitor of osteoblast proliferation and differentiation. Osteocytes decrease the synthesis of sclerostin upon mechanical

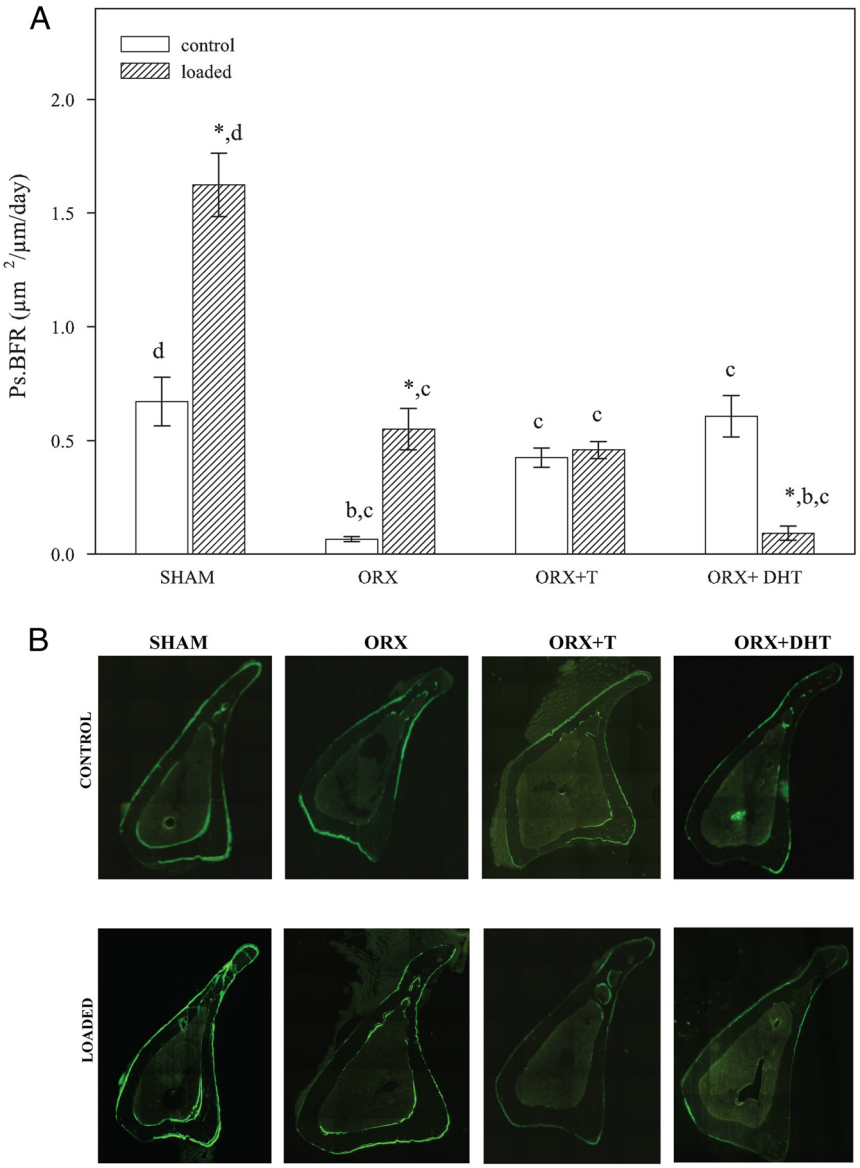

Figure 3. A, Long term effect of loading on periosteal bone formation rate (Ps.BFR/B.Pm.) was assessed ex vivo after 2 weeks of loading. B, Representative calcein images. Values are expressed as means ± SEM, n= 7–11 mice/group. $^{*}P < .05$ vs control limb, $^{b}P < .05$ vs sham control, $^{c}P < .05$ vs sham loaded, $^{d}P < .05$ vs ORX control by Repeated measures ANOVA to assess interaction between treatment and loading followed by Fisher's least significant differences multiple comparison test.

loading to promote bone formation (46). Interestingly, our study shows that the number of sclerostin positive osteocytes is also respectively decreased and increased by endogenous androgen deficiency and exogenous replacement (but not serum sclerostin) in cortical bone. This response of sclerostin to androgen deficiency and replacement was similar or even greater than the change observed during loading in sham mice. In addition, loading no longer suppressed the high sclerostin expression induced by ORX+T, whereas the already low levels in ORX were not further suppressed by loading. Recently ovariectomy (OVX) was also unexpectedly associated with low osteocyte sclerostin, without similar effects on serum sclerostin. It was hypothesized that this reduction of sclerostin may be related to greater bone formation following OVX (47). However, the response to loading was not affected by OVX in another study (24). The observation that in our study serum sclerostin did not correlate with sclerostin expression locally in bone (Figure 6A and C) was not surprising since earlier studies in animal models (47) and more recently in humans (48) showed similar discordances. In ARKO mice, osteocyte sclerostin expression decreased even more than in WT mice following loading, which is in line with our hypothesis that AR signaling limits the sclerostin suppression by loading and the subsequent osteogenic response (25). We recently observed a parallel mechanism in muscle, where AR signaling directly upregulates myostatin as a negative feedback mechanism on the anabolic effects of androgens on muscle (49). The direct target genes of AR in bone cells remain poorly understood (50), but our findings of cortical and trabecular bone gains despite sclerostin upregulation suggest that the Wnt-inhibitor sclerostin does not lie in the pathway by which AR promotes osteogenesis. A similar

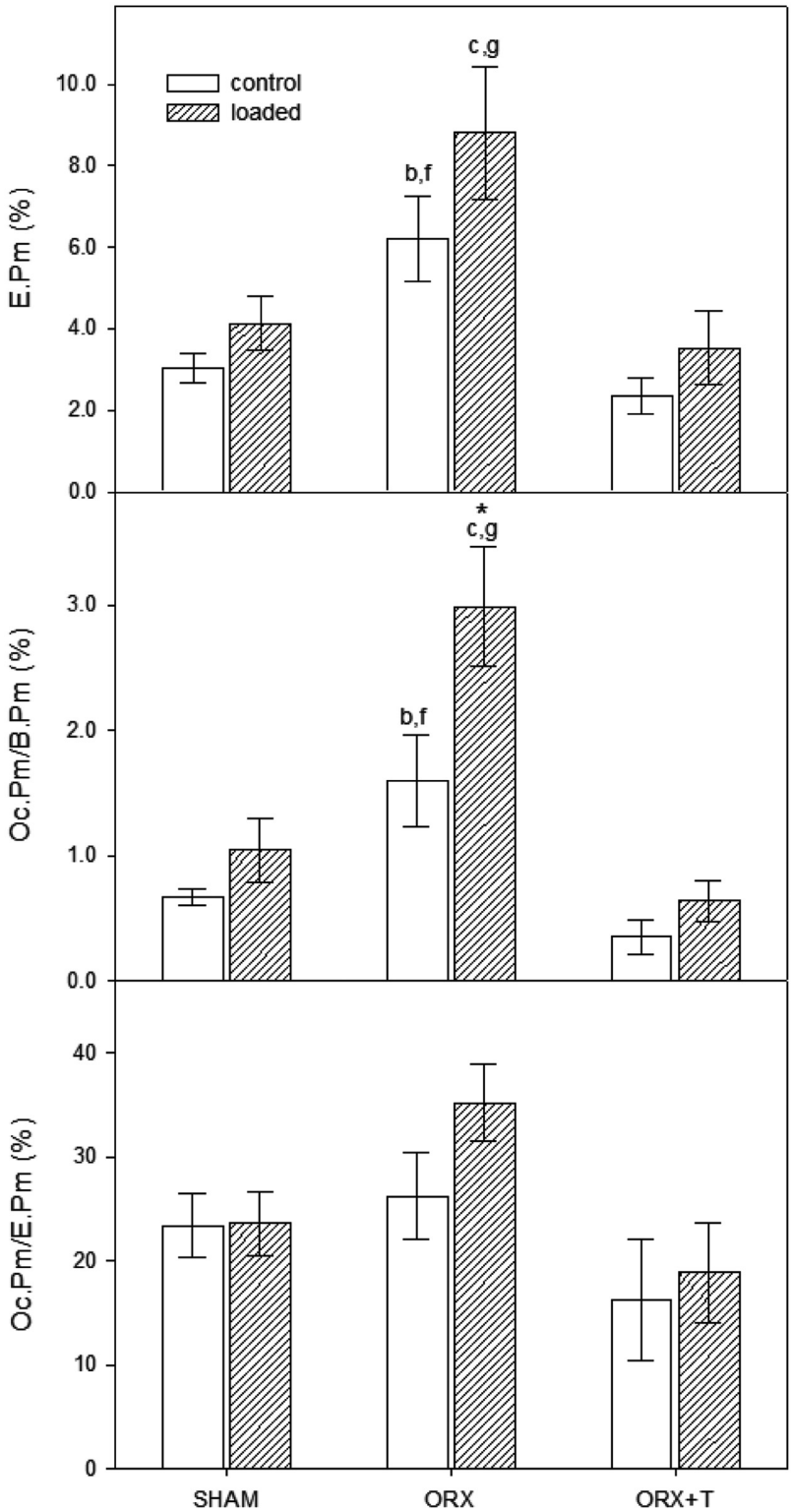

Figure 4. Long term effects of loading on osteoclast parameters in sham, ORX and ORX+T mice. Eroded perimeter (E.Pm), osteoclast perimeter per bone perimeter (Oc.Pm/B.Pm) and osteoclast perimeter per eroded perimeter (Oc.Pm/E.Pm). Values are expressed as means ± SEM, n = 3–6 mice/group. $^{*}P < .05$ vs control limb, $^{b}P < .05$ vs sham control, $^{c}P < .05$ vs sham loaded, $^{f}P < .05$ vs ORX+T control, $^{g}P < .05$ vs ORX+T loaded by Repeated measures ANOVA to assess interaction between treatment and loading followed by Fisher's least significant differences multiple comparison test.

observation has been made for ERα, which induces PI3K/AKT-dependent but Wnt/LRP5-independent activation of β-catenin signaling in osteoblastic cells (51).

As expected, we observed an increase in eroded surface and osteoclast perimeter after ORX, which was totally prevented by T replacement. Interestingly, loading further increased bone resorption in ORX mice. Therefore, the increased osteogenic response to external mechanical stress during androgen depletion was not due to a loading-induced decrease in resorption. Rather, our findings suggest that ORX increased the osteogenic response to loading by increasing bone turnover/remodeling space. In other words, loading after ORX exacerbated both bone formation and resorption, having a more pronounced effect in formation since the net result was a gain in cortical and trabecular bone volume.

The inhibitory action of T on bone formation during loading is paradoxical since androgens stimulate periosteal bone expansion and are major determinants of skeletal sexual dimorphism in cortical bone size (52). Although our study again confirms the direct actions of androgens on periosteal bone formation (27), the target cell for this effect remains unclear from conditional cell-specific ARKO models (53). Although osteocytes are thought to play a central role in coordinating bone's adaptation to mechanical loading, others and we recently showed in osteocyte-specific (Dmp1-Cre driven) models that neither osteocytic AR in males nor ERα in females regulates skeletal mechanoresponsiveness (54, 55). Therefore, the inhibition of mechanoresponsiveness may rely on AR actions in osteoprogenitor cells, periosteal cell populations or extraskeletal cells or alternatively, may represent an indirect effect of interactions between AR and other pathways such as Wnt/β-catenin. Further mecha-

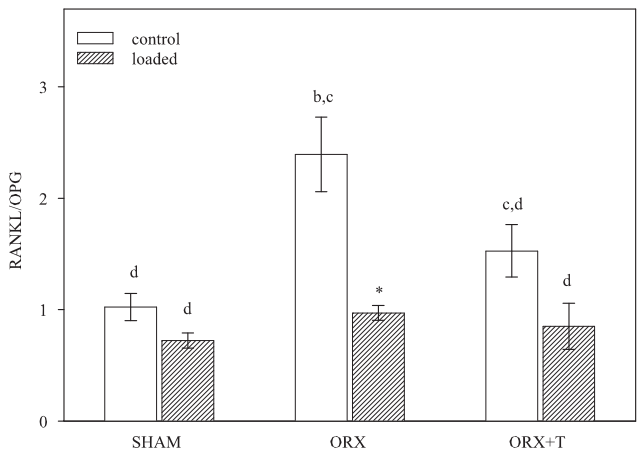

Figure 5. Short term effect of loading on relative mRNA expression levels of receptor activator of nuclear factor κ-B ligand (*Rankl*) and osteoprotegerin (*Opg*) 24 hours after one single loading in sham, ORX and ORX+T mice. Expression levels were normalized for *hypoxanthine-guanine phosphoribosyl transferase* (*HPRT*) expression. Values are expressed as means ± SEM, $n = 7–11$ mice/group. $^{*}P < .05$ vs control limb, $^{b}P < .05$ vs sham control, $^{c}P < .05$ vs sham loaded, $^{d}P < .05$ vs ORX control, $^{e}P < .05$ vs ORX loaded by Repeated measures ANOVA to assess interaction between treatment and loading followed by Fisher's least significant differences multiple comparison test.

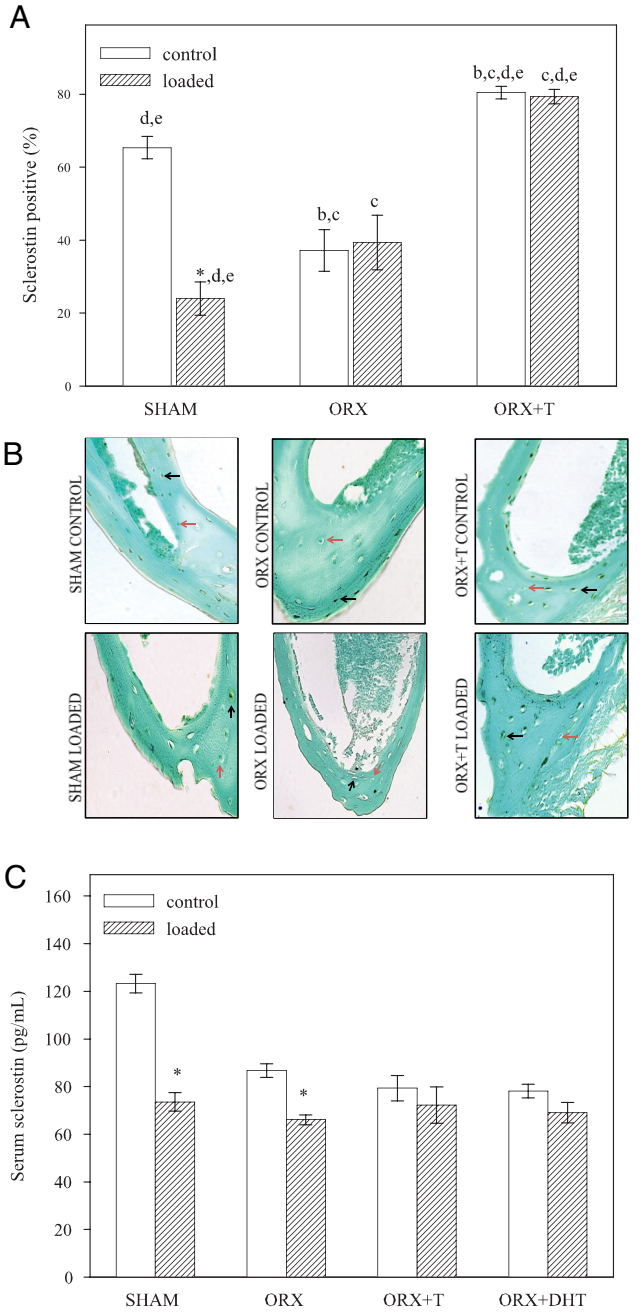

Figure 6. Short term effect of loading on load-induced changes in (A) the number of sclerostin positive osteocytes 24 hours after one single loading in sham, ORX and ORX+T mice of the total fibula. B, Sclerostin immunohistochemistry. The black arrows indicate sclerostin-positive osteocytes, whereas the red arrows show sclerostin-negative osteocytes. C, Serum sclerostin. Values are expressed as means ± SEM, $n = 7–11$ mice/group. $^{*}P < .05$ vs control limb, $^{b}P < .05$ vs sham control, $^{c}P < .05$ vs sham loaded, $^{d}P < .05$ vs ORX control, $^{e}P < .05$ vs ORX loaded by Repeated measures ANOVA to assess interaction between treatment and loading followed by Fisher's least significant differences multiple comparison test.

nistic studies are needed to investigate loading responses in cell-specific ARKO models. Sexual dimorphism has previously been noted in mice with various disruptions of the Wnt/β-catenin pathways (56), but whether sex steroids are involved also requires further investigation.

Our study, like similar previous preclinical mouse studies in this domain, has several limitations. One could hypothesize that the increased response to loading in ORX animals compared to sham is due to baseline alterations in skeletal microarchitecture occurring between castration and start of the loading interventions. Indeed, 10 days after ORX, mice already had a decreased cortical area and thickness as well as decreased trabecular bone volume and thickness at the beginning of the loading (data not shown). Although the strain gauges were measured after 10 days of castration and indicated no systematic differences between sham and ORX, strain gauges are only measured at one cortical site and provide no information about trabecular strain distribution. We therefore performed an additional experiment (long term loading*) where the same loading protocol was initiated already after 1 day of surgery, which reassuringly led to similar loading responses (Supplemental Table 3 and Supplemental Figure 1). These animal data may be important for hypogonadal men for several reasons. First, T replacement in combination with skeletal loading may diminish -not enhance- cortical bone strength gains in hypogonadal men who often have decreased cortical dimensions. Moreover, it is unlikely that the well-established stimulatory effect of T on PsBFR is related to altered skeletal mechanoresponsiveness. Conversely, it should not be assumed that bone of hypogonadal men would be less responsive to rehabilitation or physical exercise interventions. This fits with our previous observations that physical exercise may reverse some of the deleterious effects of AR disruption on the male skeleton (57). This is different to the effects of androgens and physical exercise, which have been shown to synergistically increase muscle mass and strength in elderly men (16). Secondly, an antisclerostin monoclonal antibody has recently shown promise as an osteoanabolic therapy in postmenopausal osteoporosis (58). Our study suggests that hypogonadal men may already have baseline low osteocytic sclerostin expression, which may diminish the subsequent skeletal response to antisclerostin therapy. Conversely, combination therapy with antisclerostin antibodies and T replacement may remove negative feedback on bone formation induced by T replacement, thus improving skeletal effects of the latter strategy.

In conclusion, androgens decrease the net-osteogenic response to mechanical loading in both cortical and cancellous bone of adult male mice. This decreased response to loading is due to decreased bone formation associated with early increase of osteocyte sclerostin expression. Carefully designed interventional studies in older men are needed to determine the optimal combination of endocrine and mechanical stimuli required to promote musculoskeletal mass and function and reduce fracture risk.

Acknowledgments

This study was funded by grant OT/09/035 and GOA/15/017 from KU Leuven and grant number G.0858.11 from the Research Foundation Flanders (FWO). M.R.L. and V.D. are PhD fellows of the Research Foundation Flanders. P.D. was funded by a Veterinary Research Entry Fellowship throught the Wellcome Trust. D.V. is senior investigator of the University Hospitals Leuven Clinical Research Fund.

The authors thank E. Van Herck, K. Moermans, R. Van Looveren and R. Bollen for their excellent technical assistance. We also thank the lab of J. Price (School of veterinary science, University of Bristol, Bristol, United Kingdom) for help with strain gauges and sclerostin immunohistochemistry.

Address all correspondence and requests for reprints to: Prof. Dirk Vanderschueren, Klinische en Experimentele Endocrinologie, KU Leuven, O&N I Herestraat 49 - bus 902, 3000 Leuven, Belgium, Phone: +32 16 3 46 987, Fax: +32 16 346 989, email: dirk.vanderschueren@med.kuleuven.be.

Disclosure Summary: The authors have nothing to disclose
This work was supported by .

References

1. **Khosla S, Amin S, Orwoll E.** Osteoporosis in men. *Endocr Rev*. 2008;29(4):441–464.
2. **Boonen S, Reginster JY, Kaufman JM, Lippuner K, Zanchetta J, Langdahl B, Rizzoli R, Lipschitz S, Dimai HP, Witvrouw R, Eriksen E, Brixen K, Russo L, Claessens F, Papanastasiou P, Antunez O, Su G, Bucci-Rechtweg C, Hruska J, Incera E, Vanderschueren D, Orwoll E.** Fracture risk and zoledronic acid therapy in men with osteoporosis. *N Engl J Med*. 2012;367(18):1714–1723.
3. **Laurent M, Gielen E, Claessens F, Boonen S, Vanderschueren D.** Osteoporosis in older men: recent advances in pathophysiology and treatment. *Best Pract Res Clin Endocrinol Metab*. 2013;27(4):527–539.
4. **Bhasin S, Jasuja R.** Selective androgen receptor modulators as function promoting therapies. *Curr Opin Clin Nutr*. 2009;12(3):232–240.
5. **Gielen E, Verschueren S, O'Neill TW, Pye SR, O'Connell MD, Lee DM, Ravindrarajah R, Claessens F, Laurent M, Milisen K, Tournoy J, Dejaeger M, Wu FC, Vanderschueren D, Boonen S.** Musculoskeletal frailty: a geriatric syndrome at the core of fracture occurrence in older age. *Calcif Tissue Int*. 2012;91(3):161–177.
6. **Tajar A, Huhtaniemi IT, O'Neill TW, Finn JD, Pye SR, Lee DM, Bartfai G, Boonen S, Casanueva FF, Forti G, Giwercman A, Han TS, Kula K, Labrie F, Lean ME, Pendleton N, Punab M, Vanderschueren D, Wu FC.** Characteristics of androgen deficiency in late-onset hypogonadism: results from the European Male Aging Study (EMAS). *J Clin Endocrinol Metab*. 2012;97(5):1508–1516.
7. **Mellstrom D, Johnell O, Ljunggren O, Eriksson AL, Lorentzon M,**

Mallmin H, Holmberg A, Redlund-Johnell I, Orwoll E, Ohlsson C. Free testosterone is an independent predictor of BMD and prevalent fractures in elderly men: MrOS Sweden. *J Bone Miner Res*. 2006; 21(4):529–535.

8. **LeBlanc ES, Nielson CM, Marshall LM, Lapidus JA, Barrett-Connor E, Ensrud KE, Hoffman AR, Laughlin G, Ohlsson C, Orwoll ES.** The effects of serum testosterone, estradiol, and sex hormone binding globulin levels on fracture risk in older men. *J Clin Endocrinol Metab*. 2009;94(9):3337–3346.
9. **Cauley JA, Ewing SK, Taylor BC, Fink HA, Ensrud KE, Bauer DC, Barrett-Connor E, Marshall L, Orwoll ES, M OFMS.** Sex Steroid Hormones in Older Men: Longitudinal Associations with 4.5-Year Change in Hip Bone Mineral Density-The Osteoporotic Fractures in Men Study. *J Clin Endocr Metab*. 2010;95(9):4314–4323.
10. **Wu FC, Tajar A, Beynon JM, Pye SR, Silman AJ, Finn JD, O'Neill TW, Bartfai G, Casanueva FF, Forti G, Giwercman A, Han TS, Kula K, Lean ME, Pendleton N, Punab M, Boonen S, Vanderschueren D, Labrie F, Huhtaniemi IT.** Identification of late-onset hypogonadism in middle-aged and elderly men. *N Engl J Med*. 2010;363(2):123–135.
11. **Kamerow D.** Getting your "T" up. *Bmj-Brit Med J*. 2014;348.
12. **Bhasin S, Storer TW, Berman N, Callegari C, Clevenger B, Phillips J, Bunnell TJ, Tricker R, Shirazi A, Casaburi R.** The effects of supraphysiologic doses of testosterone on muscle size and strength in normal men. *N Engl J Med*. 1996;335(1):1–7.
13. **Vanderschueren D, Vandenput L, Boonen S, Lindberg MK, Bouillon R, Ohlsson C.** Androgens and bone. *Endocr Rev*. 2004;25(3): 389–425.
14. **Finkelstein JS, Yu EW, Burnett-Bowie SAM.** Gonadal Steroids and Body Composition, *Strength, and Sexual Function in Men. New Engl J Med*. 2013;369(25):2457–2457.
15. **Snyder PJ, Ellenberg SS, Cunningham GR, Matsumoto AM, Bhasin S, Barrett-Connor E, Gill TM, Farrar JT, Cella D, Rosen RC, Resnick SM, Swerdloff RS, Cauley JA, Cifelli D, Fluharty L, Pahor M, Ensrud KE, Lewis CE, Molitch ME, Crandall JP, Wang C, Budoff MJ, Wenger NK, Mohler ER, 3rd, Bild DE, Cook NL, Keaveny TM, Kopperdahl DL, Lee D, Schwartz AV, Storer TW, Ershler WB, Roy CN, Raffel LJ, Romashkan S, Hadley E.** The Testosterone Trials: Seven coordinated trials of testosterone treatment in elderly men. *Clin Trials*. 2014;11(3):362–375.
16. **Bhasin S, Storer TW, Berman N, Yarasheski KE, Clevenger B, Phillips J, Lee WP, Bunnell TJ, Casaburi R.** Testosterone replacement increases fat-free mass and muscle size in hypogonadal men. *J Clin Endocrinol Metab*. 1997;82(2):407–413.
17. **Giannoulis MG, Martin FC, Nair KS, Umpleby AM, Sonksen P.** Hormone replacement therapy and physical function in healthy older men. Time to talk hormones? *Endocr Rev*. 2012;33(3):314–377.
18. **Price JS, Sugiyama T, Galea GL, Meakin LB, Sunters A, Lanyon LE.** Role of endocrine and paracrine factors in the adaptation of bone to mechanical loading. *Curr Osteoporos Rep*. 2011;9(2):76–82.
19. **Frost HM.** Bone's mechanostat: A 2003 update. *Anat Rec Part A*. 2003;275A(2):1081–1101.
20. **Ducher G, Bass SL, Saxon L, Daly RM.** Effects of Repetitive Loading on the Growth-Induced Changes in Bone Mass and Cortical Bone Geometry: A 12-Month Study in Pre/Peri- and Postmenarcheal Tennis Players. *J Bone Miner Res*. 2011;26(6):1321–1329.
21. **Rubin CT, Bain SD, McLeod KJ.** Suppression of the osteogenic response in the aging skeleton. *Calcif Tissue Int*. 1992;50(4):306–313.
22. **Lee KC, Jessop H, Suswillo R, Zaman G, Lanyon LE.** The adaptive response of bone to mechanical loading in female transgenic mice is deficient in the absence of oestrogen receptor-alpha and -beta. *J Endocrinol*. 2004;182(2):193–201.
23. **Lee K, Jessop H, Suswillo R, Zaman G, Lanyon L.** Endocrinology: bone adaptation requires oestrogen receptor-alpha. *Nature*. 2003; 424(6947):389.
24. **Windahl SH, Saxon L, Borjesson AE, Lagerquist MK, Frenkel B, Henning P, Lerner UH, Galea GL, Meakin LB, Engdahl C, Sjogren K, Antal MC, Krust A, Chambon P, Lanyon LE, Price JS, Ohlsson C.** Estrogen receptor-alpha is required for the osteogenic response to mechanical loading in a ligand-independent manner involving its activation function 1 but not 2. *J Bone Miner Res*. 2013;28(2):291–301.
25. **Callewaert F, Bakker A, Schrooten J, Van Meerbeek B, Verhoeven G, Boonen S, Vanderschueren D.** Androgen receptor disruption increases the osteogenic response to mechanical loading in male mice. *J Bone Miner Res*. 2010;25(1):124–131.
26. **Saxon LK, Galea G, Meakin L, Price J, Lanyon LE.** Estrogen receptors alpha and beta have different gender-dependent effects on the adaptive responses to load bearing in cancellous and cortical bone. *Endocrinology*. 2012;153(5):2254–2266.
27. **Venken K, De Gendt K, Boonen S, Ophoff J, Bouillon R, Swinnen JV, Verhoeven G, Vanderschueren D.** Relative impact of androgen and estrogen receptor activation in the effects of androgens on trabecular and cortical bone in growing male mice: a study in the androgen receptor knockout mouse model. *J Bone Miner Res*. 2006; 21(4):576–585.
28. **Vanderschueren D, Vandenput L, Boonen S, Van Herck E, Swinnen JV, Bouillon R.** An aged rat model of partial androgen deficiency: prevention of both loss of bone and lean body mass by low-dose androgen replacement. *Endocrinology*. 2000;141(5):1642–1647.
29. **Vandenput L, Boonen S, Van Herck E, Swinnen JV, Bouillon R, Vanderschueren D.** Evidence from the aged orchidectomized male rat model that 17 beta-estradiol is a more effective bone-sparing and anabolic agent than 5 alpha-dihydrotestosterone. *J Bone Miner Res*. 2002;17(11):2080–2086.
30. **Sugiyama T, Galea GL, Lanyon LE, Price JS.** Mechanical loading-related bone gain is enhanced by tamoxifen but unaffected by fulvestrant in female mice. *Endocrinology*. 2010;151(12):5582–5590.
31. **Sugiyama T, Price JS, Lanyon LE.** Functional adaptation to mechanical loading in both cortical and cancellous bone is controlled locally and is confined to the loaded bones. *Bone*. 2010;46(2):314–321.
32. **Sugiyama T, Saxon LK, Zaman G, Moustafa A, Sunters A, Price JS, Lanyon LE.** Mechanical loading enhances the anabolic effects of intermittent parathyroid hormone (1–34) on trabecular and cortical bone in mice. *Bone*. 2008;43(2):238–248.
33. **Callewaert F, Venken K, Ophoff J, De Gendt K, Torcasio A, van Lenthe GH, Van Oosterwyck H, Boonen S, Bouillon R, Verhoeven G, Vanderschueren D.** Differential regulation of bone and body composition in male mice with combined inactivation of androgen and estrogen receptor-alpha. *FASEB journal : official publication of the Federation of American Societies for Experimental Biology*. 2009;23(1):232–240.
34. **Bouxsein ML, Boyd SK, Christiansen BA, Guldberg RE, Jepsen KJ, Muller R.** Guidelines for assessment of bone microstructure in rodents using micro-computed tomography. *J Bone Miner Res*. 2010; 25(7):1468–1486.
35. **Lieben L, Benn BS, Ajibade D, Stockmans I, Moermans K, Hediger MA, Peng JB, Christakos S, Bouillon R, Carmeliet G.** Trpv6 mediates intestinal calcium absorption during calcium restriction and contributes to bone homeostasis. *Bone*. 2010;47(2):301–308.
36. **Daci E, Verstuyf A, Moermans K, Bouillon R, Carmeliet G.** Mice lacking the plasminogen activator inhibitor 1 are protected from trabecular bone loss induced by estrogen deficiency. *J Bone Miner Res*. 2000;15(8):1510–1516.
37. **Parfitt AM, Drezner MK, Glorieux FH, Kanis JA, Malluche H, Meunier PJ, Ott SM, Recker RR.** Bone histomorphometry: standardization of nomenclature, symbols, and units. Report of the ASBMR Histomorphometry Nomenclature Committee. *J Bone Miner Res*. 1987;2(6):595–610.
38. **Moustafa A, Sugiyama T, Saxon LK, Zaman G, Sunters A, Armstrong VJ, Javaheri B, Lanyon LE, Price JS.** The mouse fibula as a

suitable bone for the study of functional adaptation to mechanical loading. *Bone*. 2009;44(5):930–935.
39. **Zaman G, Jessop HL, Muzylak M, De Souza RL, Pitsillides AA, Price JS, Lanyon LL.** Osteocytes use estrogen receptor alpha to respond to strain but their ERalpha content is regulated by estrogen. *J Bone Miner Res*. 2006;21(8):1297–1306.
40. **Robling AG, Niziolek PJ, Baldridge LA, Condon KW, Allen MR, Alam I, Mantila SM, Gluhak-Heinrich J, Bellido TM, Harris SE, Turner CH.** Mechanical stimulation of bone in vivo reduces osteocyte expression of Sost/sclerostin. *J Biol Chem*. 2008;283(9):5866–5875.
41. **Tu X, Rhee Y, Condon KW, Bivi N, Allen MR, Dwyer D, Stolina M, Turner CH, Robling AG, Plotkin LI, Bellido T.** Sost downregulation and local Wnt signaling are required for the osteogenic response to mechanical loading. *Bone*. 2012;50(1):209–217.
42. **Vanderschueren D, van Herck E, Nijs J, Ederveen AG, De Coster R, Bouillon R.** Aromatase inhibition impairs skeletal modeling and decreases bone mineral density in growing male rats. *Endocrinology*. 1997;138(6):2301–2307.
43. **Chabwine JN, Talavera K, Verbert L, Eggermont J, Vanderwinden JM, De Smedt H, Van Den Bosch L, Robberecht W, Callewaert G.** Differential contribution of the Na(+)-K(+)-2Cl(-) cotransporter NKCC1 to chloride handling in rat embryonic dorsal root ganglion neurons and motor neurons. *Faseb J*. 2009;23(4):1168–1176.
44. **Fritton JC, Myers ER, Wright TM, van der Meulen MC.** Bone mass is preserved and cancellous architecture altered due to cyclic loading of the mouse tibia after orchidectomy. *J Bone Miner Res*. 2008;23(5):663–671.
45. **Beck DT, Yarrow JF, Beggs LA, Otzel DM, Ye F, Conover CF, Miller JR, Balaez A, Combs SM, Leeper AM, Williams AA, Lachacz SA, Zheng N, Wronski TJ, Borst SE.** Influence of Aromatase Inhibition on the Bone Protective Effects of Testosterone. *J Bone Miner Res*. 2014.
46. **Ke HZ, Richards WG, Li X, Ominsky MS.** Sclerostin and Dickkopf-1 as therapeutic targets in bone diseases. *Endocr Rev*. 2012;33(5):747–783.
47. **Jastrzebski S, Kalinowski J, Stolina M, Mirza F, Torreggiani E, Kalajzic I, Won HY, Lee SK, Lorenzo J.** Changes in bone sclerostin levels in mice after ovariectomy vary independently of changes in serum sclerostin levels. *J Bone Miner Res*. 2013;28(3):618–626.
48. **Roforth MM, Fujita K, McGregor UI, Kirmani S, McCready LK, Peterson JM, Drake MT, Monroe DG, Khosla S.** Effects of age on bone mRNA levels of sclerostin and other genes relevant to bone metabolism in humans. *Bone*. 2014;59:1–6.
49. **Dubois V, Laurent MR, Sinnesael M, Cielen N, Helsen C, Clinckemalie L, Spans L, Gayan-Ramirez G, Deldicque L, Hespel P, Carmeliet G, Vanderschueren D, Claessens F.** A satellite cell-specific knockout of the androgen receptor reveals myostatin as a direct androgen target in skeletal muscle. *Faseb J*. 2014.
50. **Krum SA.** Direct transcriptional targets of sex steroid hormones in bone. *J Cell Biochem*. 2011;112(2):401–408.
51. **Sunters A, Armstrong VJ, Zaman G, Kypta RM, Kawano Y, Lanyon LE, Price JS.** Mechano-transduction in osteoblastic cells involves strain-regulated estrogen receptor alpha-mediated control of insulin-like growth factor (IGF) I receptor sensitivity to Ambient IGF, leading to phosphatidylinositol 3-kinase/AKT-dependent Wnt/LRP5 receptor-independent activation of beta-catenin signaling. *J Biol Chem*. 2010;285(12):8743–8758.
52. **Callewaert F, Venken K, Kopchick JJ, Torcasio A, van Lenthe GH, Boonen S, Vanderschueren D.** Sexual dimorphism in cortical bone size and strength but not density is determined by independent and time-specific actions of sex steroids and IGF-1: evidence from pubertal mouse models. *J Bone Miner Res*. 2010;25(3):617–626.
53. **Manolagas SC, O'Brien CA, Almeida M.** The role of estrogen and androgen receptors in bone health and disease. *Nat Rev Endocrinol*. 2013;9(12):699–712.
54. **Sinnesael M, Claessens F, Laurent M, Dubois V, Boonen S, Deboel L, Vanderschueren D.** Androgen receptor (AR) in osteocytes is important for the maintenance of male skeletal integrity: evidence from targeted AR disruption in mouse osteocytes. *J Bone Miner Res*. 2012;27(12):2535–2543.
55. **Windahl SH, Borjesson AE, Farman HH, Engdahl C, Moverare-Skrtic S, Sjogren K, Lagerquist MK, Kindblom JM, Koskela A, Tuukkanen J, Divieti Pajevic P, Feng JQ, Dahlman-Wright K, Antonson P, Gustafsson JA, Ohlsson C.** Estrogen receptor-alpha in osteocytes is important for trabecular bone formation in male mice. *P Natl Acad Sci USA*. 2013;110(6):2294–2299.
56. **Mulholland DJ, Dedhar S, Coetzee GA, Nelson CC.** Interaction of nuclear receptors with the Wnt/beta-catenin/Tcf signaling axis: Wnt you like to know? *Endocr Rev*. 2005;26(7):898–915.
57. **Ophoff J, Callewaert F, Venken K, De Gendt K, Ohlsson C, Gayan-Ramirez G, Decramer M, Boonen S, Bouillon R, Verhoeven G, Vanderschueren D.** Physical activity in the androgen receptor knockout mouse: evidence for reversal of androgen deficiency on cancellous bone. *Biochem Bioph Res Co*. 2009;378(1):139–144.
58. **McClung MR, Grauer A, Boonen S, Bolognese MA, Brown JP, Diez-Perez A, Langdahl BL, Reginster JY, Zanchetta JR, Wasserman SM, Katz L, Maddox J, Yang YC, Libanati C, Bone HG.** Romosozumab in postmenopausal women with low bone mineral density. *N Engl J Med*. 2014;370(5):412–420.